OVERHEAD ELECTRICAL TRANSMISSION LINE GALLOPING
A Full Multi-Span 3-DOF Model, Some Applications and Design Recommendations

Jianwei Wang **Jean-Louis Lilien**

Montefiore Electrical Institute
University of Liège, B-4000 Liège, Belgium

Abstract - A full multi-span three-degree-of-freedom (3-DOF) iced transmission line model is presented. This new model is applicable for describing the galloping phenomena of both single and bundle lines, for performing static and dynamic analysis, and predicting the galloping behavior of iced transmission line, as well as for performing checks against field experience. Some applications for overhead transmission lines design are detailed. Some original recommendations for the design of multi-span bundle configurations are proposed.

Keywords: galloping, overhead transmission line, bundle, torsional stiffness.

1. INTRODUCTION

Galloping is a low frequency, large amplitude, wind-induced vibration of both single and bundle overhead transmission lines, with a single or a few loops of standing waves per span. It is caused by moderately strong, steady cross-wind acting upon an asymmetrically-iced conductor surface. The ice accretion on the conductor has the effect of modifying the cross-sectional shape of the conductor, so that it becomes aerodynamically unstable. The large amplitudes are generally - but not always - in a vertical plane, and range typically from $\pm$ 0.1 to $\pm$ 1.0 times the sag of the span. Frequencies are dependent on the type of line construction and the oscillation mode excited. For a typical EHV construction, frequencies usually range from 0.15 Hz to 1.0 Hz. Winds approximately normal to the line with a speed above 7 m/s are usually required and it can not be assumed that there is necessarily an upper speed limit.

Because the galloping amplitudes may approach or even exceed the sag of the span, the distances between phases become too small and phase-to-phase flashovers occur. The conductors are damaged by the power arc. Indeed, the line can be removed from service by the utility.

When galloping occurs, the strings and towers are subjected to high dynamic stress leading to mechanical damages, such as loosening and ejection of tower bolts, wear on landing bolts, ovalling of holes and distortion of tower swivels and associated hardware. Galloping can also cause the fatigue of conductor at semi-tension strings and jumpers, and of tower steelwork during sustained events. In addition, when the electrical damage happens, damage to insulator pins, spacers and Stockbridge dampers, to subconductor strands at suspension clamps and spacer clamps from fault current equalization within the bundle can also occur.

Galloping necessitates high average annual cost for repairs, for building lines to have large clearance, as well as for the installation of control devices. This cost is additional to the loss of revenue during the servicing. Moreover, several million dollars may be spent every ten years when a particularly severe example of galloping occurs and causes the collapse of lines and towers.

PE-878-PWRD-0-06-1997 A paper recommended and approved by the IEEE Transmission and Distribution Committee of the IEEE Power Engineering Society for publication in the IEEE Transactions on Power Delivery. Manuscript submitted December 30, 1996; made available for printing June 9, 1997.

State-of-the-Art

Galloping of iced conductors has been a design and operating problem since early this century. In 1930, Davidson [3] attributed the occurrence of galloping during freezing rain storms to the change in the aerodynamic lift when the wind blows across an iced conductor. Two years later, Den Hartog presented the mathematical description of the galloping mechanism – the classical aerodynamic instability criterion [5].

Progress, both in the analytical attack on the problem and in the development of countermeasures, has been slow. Sixty years after the publication of Den Hartog's analysis, important questions remain as to which variables and mechanisms are significant, and the validation of theories of galloping is still not satisfactory. No practical protection method has been developed that is recognized as fully-reliable. The slow progress has resulted from several reasons. Galloping is difficult to study in nature because of its sporadic occurrence, both in time and location. Quantitative data are difficult and sometimes risky to obtain. The varied character of ice deposits from one occasion to another makes generalization of a few observations unreliable.

Theoretical studies for galloping are greatly complicated by its dependence on nonlinear geometry, the time varying nature of the aerodynamic loads, the interactions between vertical, transversal and torsional motions, the conductors and supporting hardware as well as between adjacent spans. In addition, the unknown variation of ice accumulation and a changing wind along a conductor add further complexities. Therefore, theoretical studies have concentrated mostly on deterministic investigations which may be categorized as analytical or numerical.

Den Hartog's approach [5] takes only the aerodynamic properties of the ice profile into account. He proposed that sustained vibrations happen when the negative slope of the lift coefficient versus the wind's relative angle of attack exceeds the drag coefficient. The mechanical characteristics

of the system, the conductor torsion in particular, are excluded from that theory, at least as concerns aerodynamic effects [10, 15]. It has been suggested [7, 16, 17, 18] that the influence of the twisting of a conductor may also be significant in the initiation of galloping. Nigol and Buchan [16] emphasized the importance of the twisting. By performing wind-tunnel experiments, they concluded that the galloping of a naturally iced line is caused by a flutter instability rather than by a Den Hartog type of instability. In fact, measurements carried out on real ice profiles [2, 7, 11, 16, 19] suggested that the Den Hartog condition holds only for very slightly eccentric sheaths with lift properties opposite to those of more markedly eccentric profiles, at least for near zero angle of attack (the vector joining the centers of gravity of sheath and conductor is nearly parallel to the transversal wind direction). This type of profile generally appears as a result of freezing rain and its aerodynamic pitching moment coefficient is negligible. Furthermore, it has been suspected that a lateral (out-of-plane) motion of the conductor may be important to the initiation of galloping [21]. This phenomenon was observed by Davis *et al* [4] on a bare conductor.

The majority of previous studies on galloping were performed in a 2-DOF system (vertical and torsion) [1, 20, 24]. Even in a 3-DOF system (transversal in addition), the existing theories usually neglect some second order couplings and are only sufficient to explain the galloping of the single conductors, not that of bundle ones [8, 16, 25]. To date, very few developments on both stability and time response analysis have been performed, especially on bundle conductors.

Although the finite element approach is straightforward in principle, conventional time-stepping computations to find a steady state amplitude of galloping can be extraordinarily protracted. Because of the tediousness of parametric calculations, it is much easier to understand the physics and to obtain a better grasp of the phenomena by simplified approaches rather than by finite element ones. Therefore, a more effective approach needs to be developed to provide tools for analyzing galloping and to find more effective control devices.

This full multi-span 3-DOF model [22] can be described by a relatively simple mathematical model but which is able to describe the galloping phenomena as fully as possible, for both single and bundle conductors and both dead-end and multi-span sections, including a new theory of torsional stiffness, while taking into account the basic parameters and couplings which were neglected in other existing theories [16, 17, 25]. Some theoretical and experimental comparisons have been made with this new theory [22]. The new model correlates well with the published experimental results, test line results and actual, full-scale field tests. The simulation results of torsional stiffness coincide with the experiments to a very high degree of accuracy.

2. A Full Multi-Span 3-DOF Model

2.1 Hypotheses

Most of observed galloping takes the form of *standing waves*. The standing waves may occur with one, two or as many as ten loops in a span. Data on observed galloping of operating lines shows that the observed distribution of four or more loops is only about 2%. Therefore, for actual typical spans (span length up to 400 m), an approach by one, two and three harmonic sine waves with the possible mixing faithfully reproduces practical observations.

The mechanical behavior of overhead transmission lines is basically ruled by tension calculations. Due to the fact that the sag is only $2-4\%$ of the span length, *the tension along a span can be considered independent of the abscissa.* The suspension insulator is considered as a rigid body which can move only in a longitudinal direction.

As most of the actual attachments of bundle conductors at *suspension clamps*, the relative longitudinal movement between subconductors is free (within several centimeters). This has the effects on torsional stiffness of a multi-span section.

The *anchoring attachment* points are considered without vertical, transversal nor torsional motions. The anchoring attachment in torsion is defined by a flexibility matrix which is easily managed for most practical cases by the knowledge of yoke plate design.

The *towers* are considered as springs. Because the tower frequency is generally higher than 1 Hz (which is higher than galloping frequency), the tower anchoring stiffness is approximated by its static behavior. The dynamic behavior of towers are not considered.

Subconductors are uniformly distributed along the circumferential geometry.

The *bundle* is found out by an equivalent single conductor that presents similar mechanical behavior to that of a bundle of any number of subconductors (similar as used by Yamaoka [23]). The main differences with single conductor are from torsional stiffness.

Ice accretion is presumed to be received instantaneously on the conductor all along the span under no-wind condition, i.e. the same ice shape all along the span. Thus the ice accretion is defined by one angle which is in fact the angle at the anchoring or suspension point, independent of wind condition. Due to the bundle stiffness, ice pendulum effect, blow-back angle, and aerodynamic pitching moment, the ice position which is a function of ice shape and wind speed varies finally all along the span. Aerodynamic properties on each subconductor are considered the same.

2.2 The Brief Mechanism of Galloping

Galloping is always caused by moderately strong, steady crosswind acting upon an asymmetrically iced conductor surface. This asymmetry generally appears when the meteorological conditions are favorable for the formation of ice coating around the conductors which grows preferentially on the side facing the wind or the precipitation.

The origin of galloping is caused by two aerodynamic forces due to wind action on an asymmetrical conductor profile. *Because of the boundary conditions, the cable can rotate only around its shear center.* The aerodynamic drag and lift acting in the aerodynamic center are replaced by three aerodynamic loads acting in the shear center of the cable: the drag f_D, the lift f_L and an additional pitching moment M_W. The drag and lift forces are respectively parallel and perpendicular to the relative wind speed vector which refers to conductor movement. The reference direc-

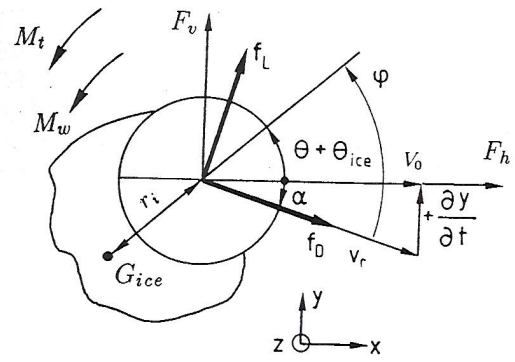

Figure 1: Definition diagram of angles and forces (angles and moments are anticlockwise positive.)

tions are defined in Fig. 1, where V_r is the relative wind speed.

For some appropriate ice accretion angle θ_{ice}, the aerodynamic coefficients behave in such a way that upwards velocity increases the vertical force and that downwards velocity decreases the vertical force. The drag damping effect can be so compensated that a self-sustained oscillation appears. This oscillation is known as *galloping*.

2.3 The Multi-Span Line System

The vertical, transversal and torsional motion of the line system can be described by the following second-order partial derivatives equations:

$$\begin{cases} m\dfrac{\partial^2 y}{\partial t^2} + C_y\dfrac{\partial y}{\partial t} - T\dfrac{\partial^2 y}{\partial z^2} = F_v(z) \\ m\dfrac{\partial^2 x}{\partial t^2} + C_x\dfrac{\partial x}{\partial t} - T\dfrac{\partial^2 x}{\partial z^2} = F_h(z) \\ I\dfrac{\partial^2 \theta}{\partial t^2} + C_\theta\dfrac{\partial \theta}{\partial t} - GJ\dfrac{\partial^2 \theta}{\partial z^2} = M_t(z) \end{cases} \tag{1}$$

where y and x are respectively the displacements in the vertical and the transversal plane and where θ is the torsional angle. The definitions of angles and forces of this 3-DOF system are to be found in Fig. 1. C_y, C_x and C_θ represent the damping constants. T is related to the strains evolving from the movement of the cable (see **2.6**). GJ represents the torsional stiffness, linear for single conductors and highly nonlinear for bundles. Bundle stiffness depends on many parameters such as tension, spacer, number of subspan and flexibility matrix, etc. F_v, F_h and M_t are the excitations for the iced conductor system in 3-DOF. They act together with the aerodynamic drag, lift and moment in addition to internal inertial contributions. Furthermore, m and I are respectively the total mass and the moment of inertia of the *iced conductor's* cross-section per unit length.

Let us consider the modal decomposition of the functions $\eta(z,t)$

$$\eta(z,t) = \sum_{k=1}^{3} \eta_k(t)\sin k\beta \qquad with \quad \beta = \frac{\pi z}{L} \tag{2}$$

where η represents successively y, x and θ. t is the time, L and z are respectively the length of span to be considered and the distance between the beginning of the span and the point to be studied, k is the mode number. The 3-DOF conductor system with each specific mode k is described by

$$\begin{cases} m\dfrac{d^2 y_k}{dt^2} + C_y\dfrac{dy_k}{dt} + T\left(\dfrac{k\pi}{L}\right)^2 y_k = \dfrac{2}{\pi}\displaystyle\int_0^\pi F_v \sin k\beta d\beta \\ m\dfrac{d^2 x_k}{dt^2} + C_x\dfrac{dx_k}{dt} + T\left(\dfrac{k\pi}{L}\right)^2 x_k = \dfrac{2}{\pi}\displaystyle\int_0^\pi F_h \sin k\beta d\beta \\ I\dfrac{d^2\theta_k}{dt^2} + C_\theta\dfrac{d\theta_k}{dt} + GJ\left(\dfrac{k\pi}{L}\right)^2 \theta_k = \dfrac{2}{\pi}\displaystyle\int_0^\pi M_t \sin k\beta d\beta \end{cases} \tag{3}$$

This system is used for all spans of the section. Thus the partial differential equations can be easily solved by time integration. Nonlinear couplings exist between different spans and between different modes due to tension T, torsional stiffness GJ (for bundle conductors) and aerodynamic forces (included in F_v, F_h and M_t), which include the angle of attack.

2.4 Aerodynamic Excitations

The source of the external excitations is the wind. These external loads are the aerodynamic forces and moments. According to aerodynamics, the drag force f_D, the lift force f_L and the pitching moment M_W are given by

$$\begin{cases} f_D = K_D V_r^2 C_D(\varphi, V_r) \\ f_L = K_D V_r^2 C_L(\varphi, V_r) \\ M_W = K_M V_r^2 C_M(\varphi, V_r) \end{cases} \tag{4}$$

$$\text{with} \quad K_D = \frac{1}{2} n \rho_{air} \phi \quad \text{and} \quad K_M = \frac{1}{2} n \rho_{air} \phi^2$$

where n is the number of subconductors, ρ_{air} is the mass density of the air, V_r is the relative wind speed, ϕ is the diameter of the conductor, φ is the angle of attack (see Fig. 1). C_D, C_L and C_M represent the aerodynamic coefficients of drag, lift and moment respectively (curves obtained from wind tunnel tests).

2.5 The Angle of Attack

The angle of attack is defined as the angle between the instantaneous ice location and the apparent wind speed, as φ in Fig. 1. The angle of attack is one of the most active factors for galloping.

The wind velocities relative to the conductor in both vertical and transversal directions are described by

$$v_x = V_{0x} - r_i\frac{\partial\theta}{\partial t}\sin(\theta + \theta_0) - \frac{\partial x}{\partial t} \tag{5}$$

$$v_y = V_{0y} + r_i\frac{\partial\theta}{\partial t}\cos(\theta + \theta_0) - \frac{\partial y}{\partial t} \tag{6}$$

where θ_0 is the angle of the conductor in the original equilibrium position (generally equal to the ice accretion angle θ_{ice} for single conductors), r_i is the distance between the

shear center of the conductor and the center of gravity of the ice deposit (G_{ice}), V_{0x} and V_{0y} are the components of the absolute wind velocity V_0.

The angle of attack is given by

$$\varphi = \theta_0 + \theta - \alpha \tag{7}$$

For bundle conductors, the bundle geometry provides additional rotating contributions.

2.6 Modelling of Tension

The global tension variation is related to the total length variation induced by the motion of the cable over the *whole multi-span section*. Considering the longitudinal stiffness K_e (including the stiffness of anchoring towers), the global tension for a N-span section (whatever its configuration) is given by

$$T = T_0 + K_e \sum_{j=1}^{N} \Delta l_j \tag{8}$$

where T_0 represent the initial tension before galloping. Δl_j the length variation of the span j.

Using the modal decomposition and rectification formulae, the global tension of the cable for a multi-span section is found by

$$T = T_0 + K_e \sum_{j=1}^{N} \sum_{k=1}^{3} \frac{1}{L_j} \left(\frac{k\pi}{2}\right)^2 \left(y_{j,k}^2 - y_{j,k0}^2 + x_{j,k}^2 - x_{j,k0}^2\right) \tag{9}$$

where y_{k0} and x_{k0} are the magnitudes of the odd mode k at the static equilibrium position in the vertical and transversal plane respectively (y_{k0} and x_{k0} are null for even mode k).

Due to the configuration of multi-span overhead lines, the movement of the suspension insulator is mainly longitudinal and transversal with only a very limited movement in the vertical plane. Furthermore, the movements in both the vertical and the transversal planes have no significant influence on the length variation of the cable of the multi-span section. The sole longitudinal movement should then be kept and dealt with.

The movements of the suspension insulators affect the tension in the multi-span section. This is the main reason why tension compensates so well in some cases. Access to suspension longitudinal movement can be easily managed by separately evaluating the tension in each span, based on the longitudinal displacement of suspension insulator (Equations (8) and (9) will be slightly modified).

2.7 Bundle Torsional Stiffness

The galloping mechanism is closely related to stiffness, especially to the torsional stiffness. Up to now, due to the complexity of the bundle torsional stiffness, the existing 3-DOF theories [16, 25] are limited to the study of the galloping of single conductors, and fail to investigate this phenomenon for bundle conductors. Although there exist a few theories [6, 12, 14] for bundle conductors, they are 2-DOF and only valid for small torsional movements. In 1977, Nigol *et al* [17] presented a complete model for bundle stiffness, but showing significant discrepancies with experimental results (up to 50%). The new model introduced in this paper is valid for both small and large torsional movements of bundles until collapse. There are no more discrepancies between the simulation results by this new model and experimental results (detailed in [22]).

An Analytical Expression of Torsional Stiffness

Using the mode decomposition and considering one mode, the following global expression of the torsional stiffness can be found.

$$GJ = (\tau + r^2 T) + \frac{16r^2}{3L}\left[K_2 y_k^2 + K_1 x_k^2 - (K_3 + K_4) y_k x_k\right] \tag{10}$$

where L is the total length of spans in the whole section and r represents the radius of the bundle. K_i depends on the flexibility matrix of anchoring (related to the yoke plate assembly), the number of subconductor, bundle geometry and the sagging conditions.

The first term ($\tau + r^2 T$) of (10) is identical to Nigol theory [17] but the second one is a new term. This term can be as large as the first one so that neglecting it can lead to an under-estimation of the bundle torsional stiffness by about 50%. The second term results only from the tension differences between subconductors arising from the anchoring attachment of the bundle. The influence of this term increases as the number of spans decreases.

A Simplified Torsional Stiffness Formula

Considering small rotations, if there is no global transversal movement and no initial rotation of the bundle, the torsional stiffness can easily be obtained from (10) as

$$GJ = \tau + r^2 T_0 + \frac{16r^2 K_2}{3L} y_{k0}^2 \tag{11}$$

Twin bundles, for example, have two extreme values of torsional stiffness, i.e.:
Typical vertical twin bundle:

$$GJ = \tau + r^2 T_0 \tag{12}$$

Typical horizontal twin bundle:

$$GJ = \tau + r^2 T_0 + \frac{16r^2 EA}{3L^2} y_{10}^2 \tag{13}$$

where E represents the Young's modulus, A the cross-section of one phase. This simplified torsional stiffness formula (11) allows for the complex bundle stiffness to be directly calculated from the basic parameters.

2.8 Experimental Comparisons

Some experimental comparisons have been made with this new theory. The simulation results of torsional stiffness coincide with the experiments on both test lines and actual, full-scale lines to a very high degree of accuracy [22]. Due to the complexity of galloping, it is difficult to perform dynamic experiment of galloping. As far as the authors are aware of, the only published dynamic experimental result (with known ice shape and aerodynamic coefficients) is given by Yu *et al* [25]. This full multi-span 3-DOF model correlates well with this published experimental result [22].

3. CASE STUDIES

A two-span section of a 420 kV transmission line in Norway was subjected to galloping. The span lengths are 292 m and 196 m respectively. The basic data are: ACSR horizontal twin bundle, subconductor cross-section $A = 863.10$ mm^2, Young's modulus $E = 7.0 \times 10^{10}$ N/m^2, mass of subconductor per unit length $m = 2.879$ kg/m, subconductor diameter $\phi = 38.25$ mm, subconductor separation $d = 0.45$ m, sagging tension per subconductor $T_0 = 50802$ N, intrinsic torsional stiffness $\tau = 530$ Nm^2, 15 spacers per span. Percentage critical damping in vertical, torsion and transversal are 0.5%, 4% and 0.5% respectively.

Galloping occurred after a while under the following external conditions:

$V_0 = 15$ m/s, WIND $\Longrightarrow$, $\theta_{ice} = -50°$, ice thickness $= 6mm$

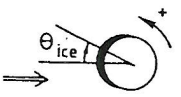

Unfortunately, there was no any recorded result during galloping.

The time evolution of galloping in the vertical, the transversal planes and in torsion at mid-span as well as the tension are simulated right from the initiation of galloping to the steady galloping. View of galloping in vertical is shown in Fig. 2.

The *limit cycle* of the time response means the steady galloping state. The time evolution at mid-span during the limit cycle is simulated for the 3-DOF and allows us to find not only the galloping amplitudes in the vertical, the transversal planes and in torsion, but also the mechanical tension (Fig. 3, Fig. 4, Fig. 5 and Fig. 6). From the limit cycle characteristics for two spans (at mid-span), it can be seen that this galloping is an "up-and-down" type of galloping (Fig. 3). The galloping ellipses at each mid-span, shown in Fig. 7, are also important results. Because of the different sag of each span in this case, galloping ellipses in Fig. 7 are shifted.

These simulation results clearly show that this two-span section is also sensible to galloping with large amplitudes, as observed in the field.

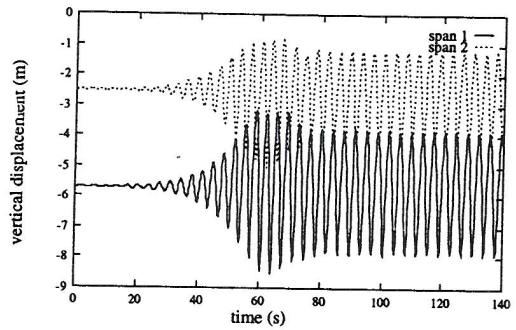

Figure 2: Time evolution of galloping in the vertical plane

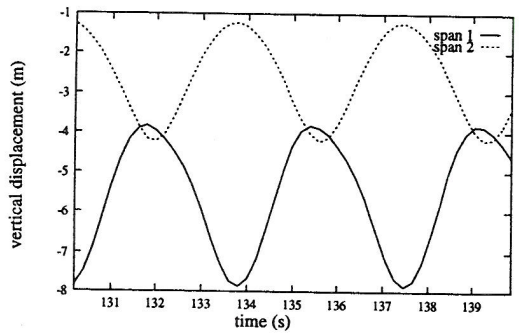

Figure 3: Time evolution of the vertical displacement (a zoom of Fig. 2, typical "up-and-down" movement)

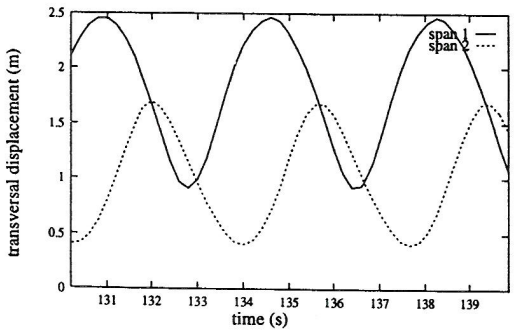

Figure 4: Time evolution of the transversal displacement

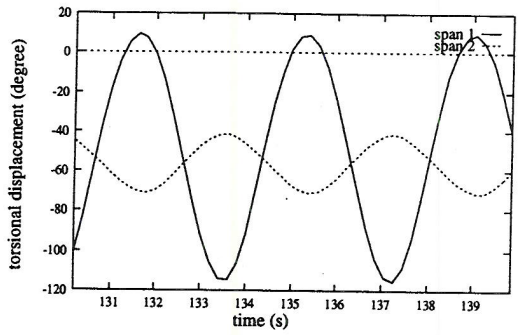

Figure 5: Time evolution of the torsional angle

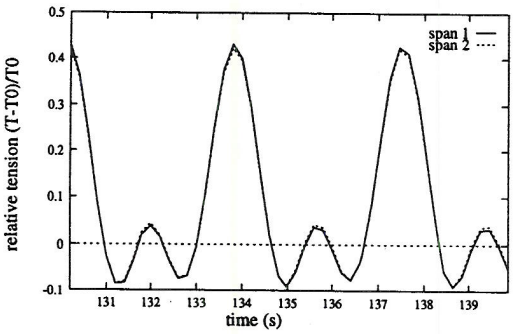

Figure 6: Time evolution of the mechanical tension resulting from the movement of the whole section

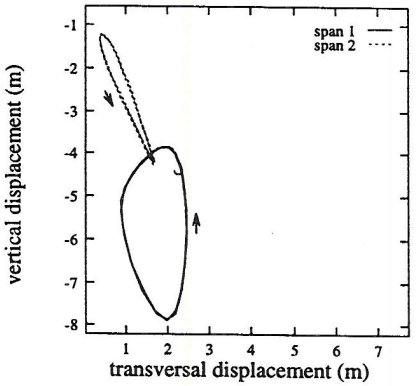

Figure 7: Galloping ellipses

4. DESIGN RECOMMENDATIONS

For large rotations, the nonlinearity of the torsional stiffness is mainly due to the differences of tension between subconductors. These tension differences evolve from the anchoring attachment of the bundle and also depend on the total number of spans. The higher the number of spans, the lower the nonlinearity of the torsional stiffness. Fig. 8 gives details on the influence of the number of spans and different suspension sets on the torsional stiffness.

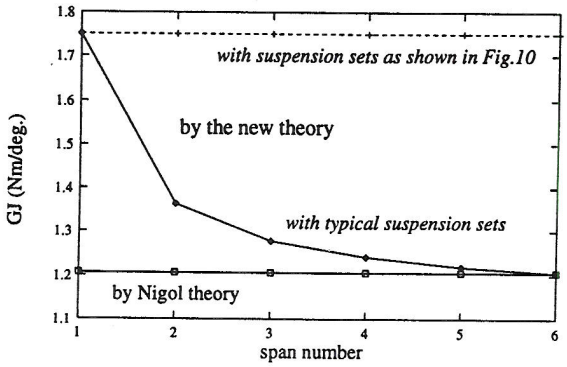

Figure 8: The influence of the number of spans on torsional stiffness in one span of a section

From Fig. 8 it can be seen that for the same set of data, *the bundle torsional stiffness of a span in a multi-span section is lower than that of a dead-end span section and depends on the number of spans in the section. The "dead-end effect" of anchoring towers tends to disappear when the number of spans is more than 4. Dead-end span sections can sometimes increase the bundle stiffness more than 50% by comparing with the same span included in a multi-span section.* This is mainly because in a multi-span section, conductors can move freely and independently in longitudinal direction at the suspension clamp locations, so that tension compensates well from one span to another.

It is possible to avoid this *relative movement* by an appropriate suspension assembly, instead of the typical suspension sets (as shown in Fig. 9). For example, Fig. 10 clearly shows this possibility.

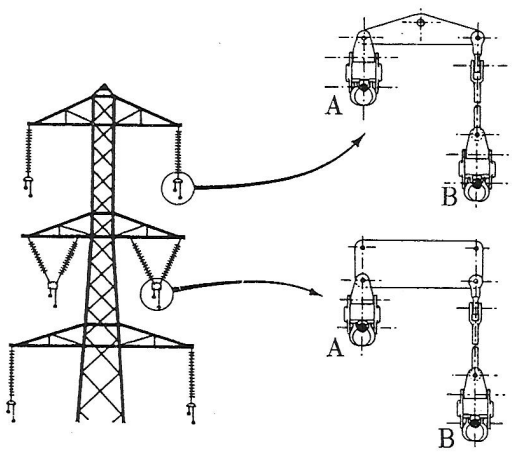

Figure 9: Typical suspension sets. Subconductors A and B can move longitudinally and independently each other in a range of several centimeters.

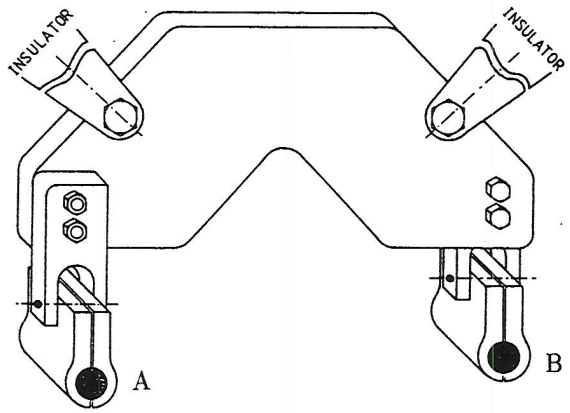

Figure 10: A new suspension assembly for V-shape insulators. Subconductors A and B can not move independently in longitudinal direction.

This is particularly important because it will shift the ratio of frequency (between vertical and torsional motions) to a significant amount. In such a case, couplings of torsional motion between spans will disappear but couplings of vertical motion between spans will still remain. By this way, "up-and-down" galloping risks of bundles will disappear in most of the cases. This is because most of galloping of bundles are aero-elastic instability (not the Den Hartog type galloping) and come from the fact that the ratio of frequency between vertical and torsional motions is generally close to 1. Such new suspension set will increase the torsional stiffness by about 50% (from 1.2 Nm/deg to about 1.8 Nm/deg) and therefore induce a detuning of about 25% by shifting up the frequency of torsional motions.

5. INVESTIGATIONS OF ANTI-GALLOPING METHODS

Some investigations have been done (based on the same Norwegian multi-span bundle case) to find the most effective anti-galloping method for bundle conductors based on this case.

5.1 Modifying the Subconductor Separation

Fig. 11 shows the results of modifying the spacing of the bundle. It can be seen that when the spacing increases, the vertical peak-to-peak amplitude keeps slowly growing and reaches a maximum for a certain value of spacing. After this specific spacing value, the vertical peak-to-peak amplitude decreases sharply to recover a stable state. This is explained by the close relation between the bundle moment of inertia and the bundle spacing. Modifying the spacing sensibly modifies the bundle moment of inertia. The bundle moment of inertia is a very sensible factor of the bundle stability.

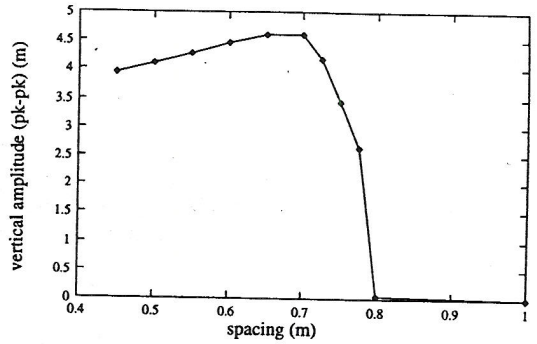

Figure 11: Galloping in the vertical plane as a function of spacing (Norwegian 2-span case, $V_0 = 15$ m/s, $\theta_{ice} = -50°$, ice thickness = 6 mm)

5.2 Employing Pendulums

The detuning pendulum (eccentric concentrated mass which can make the shifting between vertical and torsional frequencies) is one of anti-galloping devices (first used by Havard [9]). Fig. 12 illustrates the pendulum effects and displays the vertical amplitude as a function of the pendulum parameter $\sum_{p=0}^{N_p} m_p g l_p$.

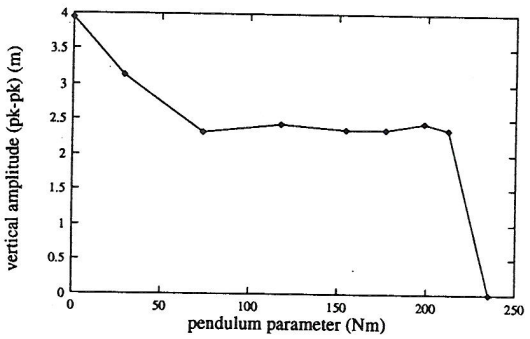

Figure 12: Galloping in the vertical plane as a function of pendulum effects: $\sum_{p=0}^{N_p} m_p g l_p$, (Norwegian 2-span case, $V_0 = 15$ m/s, $\theta_{ice} = -50°$, ice thickness = 6 mm)

The sole implementation of pendulums, for example 3 pendulums per span with $m_p g l_p = 71$ Nm per pendulum (lever arm: 0.45 m, mass: 16 kg), is not sufficient to avoid instability (in this case, at least 3 times more masses could be successful). Since the overhead line is limited in extra-weight, we suffer a limitation in the number of pendulums to install as well as in the mass of each pendulum.

5.3 The Combination of Detuning and Torsional Damping

Due to the above limitations, the simulated influence of a new anti-galloping device – TDD (torsional damper and detuner [13]) on the above mentioned Norwegian case has been calculated. Three TDDs per span are used and their characteristics are: an arm of 0.45 m, mass of 16 kg per TDD (same as the mentioned inefficient pendulums), and a torsional damping of 12% and the dimension of yoke plates is changed to 0.4 m.

The simulation results [22] show that the combination of detuning and torsional damping is a very efficient anti-galloping method and no more galloping occurs in this two-span section.

Some field tests of TDDs on twin bundle lines have been performed and good anti-galloping effects have been obtained.

6. CONCLUSIONS

This new model is a full multi-span 3-DOF model for both single and bundle conductor galloping and includes a new theory of torsional stiffness for bundle conductors valid for large rotation until collapse. All mixing between 1, 2 and 3 loop galloping can be simulated by this new model, together with all second order coupling factors between vertical, transversal and torsional modes, including movement effects of suspension insulators.

The attachment to anchoring towers by yoke plates and the attachment to suspension towers by suspension clamps play a key role in the torsional stiffness. By appropriate choice of the anchoring conditions and suspension clamps at the design stage, the bundle torsional stiffness can be easily increased so that a detuning factor between vertical frequency and torsional frequency can be obtained without any significant additional cost, which could help to avoid galloping.

Anti-galloping devices are widely used as a method to avoid galloping. This comprehensive mathematical model is a foundation for performing structural analyses for investigations of anti-galloping devices. The anti-galloping devices which combine detuning and torsional damping will be able to solve the flutter galloping problem.

The software based on this 3-DOF model can perform both static and dynamic evaluations, frequency analysis, stability analysis and the special evaluation of both single and bundle torsional stiffness. This model gives the full, time response evolutions of galloping. It can simulate the time response of amplitudes in vertical, transversal and torsional motion, tension, loads in the insulator strings, as well as the galloping ellipse. It is able to simulate any galloping behavior, all mixing between 1, 2 and 3 loops on a full section line (for any iced transmission line configuration up to 20 spans), including movement effects of suspension insulators.

Some original recommendations for design have been proposed in this paper. It can alleviate galloping and reduce galloping consequences in the design stages by the appropriate design of suspension assembly, and the sub-conductor separation. For the operating lines, installing anti-galloping devices which combine detuning and torsional damping effects is an effective method to alleviate galloping and reduce galloping consequences.

This full multi-span 3-DOF model is a very effective tool for describing the galloping phenomena, for performing static and dynamic analysis, and predicting the galloping behavior of iced conductors, as well as for performing checks against field experience. Therefore this full multi-span 3-DOF model can be used for both galloping studies and as an aid for electrical overhead transmission line design.